IEEE Access
Multidisciplinary | Rapid Review | Open Access Journal

Received 26 January 2023, accepted 25 February 2023, date of publication 2 March 2023, date of current version 7 March 2023.

Digital Object Identifier 10.1109/ACCESS.2023.3251580

THEORY

Speed-Control Technique for Achieving Fair Uplink Communications With a UAV-Aided Flying Base Station

SHU MITSUI, (Student Member, IEEE), AND HIROKI NISHIYAMA, (Senior Member, IEEE)
Graduate School of Engineering, Tohoku University, Sendai 980-8579, Japan

Corresponding author: Shu Mitsui (shu.mitsui.t8@dc.tohoku.ac.jp)

This work was supported in part by the Japan Society for the Promotion of Science KAKENHI under Grant JP20K11785.

ABSTRACT The use of aerial base stations on unmanned aerial vehicles (UAVs) is a notable solution for providing disaster victims with communication services because they can be quickly deployed immediately after a disaster. In this study, we investigate how a single circling UAV with an aerial base station can be used for collecting uplink information from users on the ground. In this system, users within the coverage area of an aerial base station share the available system bandwidth. Consequently, since a UAV's flying speed is constant, a fairness issue becomes significant among ground users distributed over the service area when their spatial density differs largely from place to place. To solve this fairness issue, we focus on a speed-control technique for the UAV. We begin by formulating the amount of transmitted data from each user equipment (UE) as a function of the communication time, during which the user is within the coverage of the aerial base station, and which depends on the speed of the UAV. The objective function can be defined as a maximization of the minimum amount of data transmitted by each UE. Then, we develop the proposed speed-control technique by analyzing the quantitative relationship between the UAV's flying speed and the amount of data transmitted by each UE. Finally, we use computer simulations to demonstrate the effectiveness of our technique.

INDEX TERMS Unmanned aerial vehicle (UAV), speed control, fairness, disaster.

I. INTRODUCTION

Unmanned aerial vehicles (UAVs) have been used in a wide variety of applications over the last few decades owing to their high mobility and low cost. In recent years, because of their increased availability, in addition to military operations their use has extended to private and commercial fields, such as observation, forest fire detection, and freight transportation because UAV is available more easily now [1]. UAVs are expected to be useful in the wireless communication field [2], and many studies have been conducted accordingly. For instance, [3], [4], [5], [6], [7], [8] sought to maximize throughput, reduce delay, and maximize energy efficiency by incorporating the UAV into terrestrial networks. Moreover, research is being conducted on how the flight-based qualities of UAVs can be used to expand coverage over the sea and to build non-terrestrial networks [9], [10], [11], [12], [13], [14]. The point is that a network generated by UAVs can be flexibly developed by changing their number, position, and trajectory. Also, a good communication environment can be achieved because UAVs can more easily communicate along the line-of-sight (LoS) [15]. One application that can make good use of these advantages is communication recovery during a disaster.

At present, communication infrastructure is dependent on wired facilities such as base stations and backhaul links. Therefore, when a disaster such as an earthquake or tsunami affects this infrastructure, mobile users inevitably lose network connectivity, making it difficult to gather information from users within the disaster-affected areas and to optimize disaster response. In other words, the loss of network connectivity is a serious problem that must be avoided as much

The associate editor coordinating the review of this manuscript and approving it for publication was Razi Iqbal.

as possible, and the demand for disaster-resilient communication systems is increasing. One of the most promising solutions to this problem is to deploy aerial base stations onboard UAVs in disaster-affected areas [16], [17], [18], [19], [20], [21].

Many communication systems using UAV swarms to cover large areas have been proposed [22], [23], such as the information collection system in [24], in which UAVs fly in a circular trajectory. Timeliness and fairness are two important aspects of information collection systems like this when they are used in disasters. Timeliness is important because collecting real-time information is essential for ensuring the smooth rescue of victims. It is evaluated by looking at the elapsed time from when information is generated by the sender to when it is passed to the receiver [25], [26], and in that model, timeliness is ensured by the constant circling period of the UAV. Fairness is important because it is necessary to collect information from as many users as possible in an area where a disaster has caused an outage in network connectivity. Consequently, it is essential to ensure fairness in users' ability to access the network, more so than in normal situations. When a UAV's flying speed is constant, an uneven spatial distribution of multiple ground-based user equipment (UE) will create an access disparity. In areas where the distribution density of UEs is large, the number of devices that must be accommodated by the UAV is also large, and, consequently, the bandwidth per UE is small. As a result, the communication volume for UEs is lower. Conversely, in areas where the distribution density of UEs is small, the communication volume for UEs is higher. To solve this problem, the speed control of UAVs needs to adapt to the distribution density of UEs. Therefore, considering timeliness and fairness, we need to develop a speed control technique that uses UAVs with a constant circling period to resolve the unfairness caused by an uneven spatial distribution of UEs. This problem also arises when using a single UAV, so in this study we focus on using a UAV as a flying base station and consider the fairness issue for users on the ground in a disaster-affected area.

The major contributions of this study can be summarized in the following points.

- We introduce a communication system that uses an aerial base station carried by a UAV flying in a circular trajectory. In this system, the service area becomes larger than the radio coverage of the base station due to the UAV's mobility.
- We identify the fairness issue caused by an uneven spatial distribution of users. We formulate the issue as an optimization problem, then develop its solution by considering the amount of data potentially transmitted by each UE, which can be derived from the geographical relation between the UAV and the UEs, and from the velocity of the UAV.
- We develop a speed-control technique that improves fairness in the amount of transmitted data among UEs with consideration of the speed limit of the UAV. It adheres to two strict conditions: the speed limit of the UAV and the turn period of the UAV.
- Using computer simulations, we confirm that the speed of the UAV changes in accordance with our proposed method and that the speed and cycle restrictions are satisfied. We also show that our method improves fairness in the amount of transmitted data among UEs.

The rest of this paper is organized as follows. Section II introduces related works and clarifies the problem that we are attempting to solve. In Section III, we describe the UAV-assisted communication system and formulate the objective function. Section IV gives an overview of our technique for controlling the flying speed of the UAV, which is used to solve the problem. In Section V, we conduct simulations to confirm the superior performance of our technique. Finally, we present our conclusions in Section VI.

II. RELATED WORKS

There are many studies that have used UAVs as aerial base stations in disaster areas. Reference [27] studied a bandwidth allocation method that took the fairness issue into account, and was used in an information collection model using a single UAV. This study differs from ours in that it focused on the unfairness caused by differences in the signal-to-noise ratio (SNR) and the transmission time for different UEs. In [28], a model with two UAVs, one hovering over the center of the affected area and the other flying in a circular trajectory along the periphery of the circular area, showed that network performance was improved by optimizing the number of channels, UAV altitude, and transmission power. Fadlullah et al. [24] took a network created by a swarm of circling UAVs and dynamically adjusted their center coordinates and orbit radius, their goal being to improve the connection probability of end-to-end communication and the communication delay. Reference [29] looked at maximizing the total rate of uplink communication across Internet-of-Things (IoT) devices and the UAV, and they co-optimized scheduling, the uplink transmit power of IoT devices, and the UAV altitude. In these studies, UAVs flew along a set trajectory at constant speed during a disaster scenario, allowing them to cover a larger area than can be achieved with stationary UAV coverage.

Additionally, several studies have worked on speed-control techniques for UAVs, and they solved the problem caused by the distribution density of network nodes on the ground. Reference [30] devised a speed-control method that maximizes the efficiency of data collection for IoT devices with consideration of the impact of the charging process. However, they only provided three patterns of UAV speeds, so it is difficult to conclude that they derived the optimum speed. Pan et al. [31] took the congestion state of a medium access control (MAC) layer into consideration and dynamically adjusted the UAVs' speed for reliable and efficient data collection. Moreover, they found that when the speed of a UAV increases to around 20 m/s, the probability of successful access for IoT devices on the ground decreases dramatically, making it

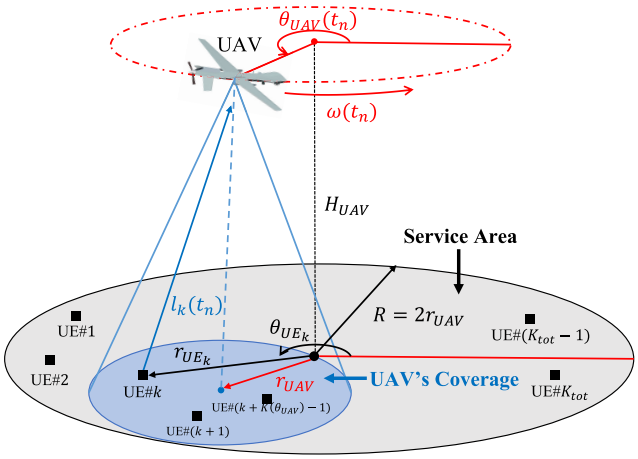

FIGURE 1. System model.

difficult to transmit data to the UAV. Reference [32] proposed a speed-control technique that minimizes the flight time for a UAV collecting data from a set of ground sensors. This study found that the speed of the UAV varies depending on the location of the sensors, the amount of data required to be transmitted by them, and their energy usage. References [33] and [34] used a system model similar to the one in [28] to solve the problem caused by the ground terminal (GT) distribution density. Reference [33] worked on maximizing the number of GTs that satisfy the constraint for the minimum amount of transmitted data by optimizing bandwidth allocation and speed. Reference [34] set up a more realistic GT distribution model based on the Thomas cluster process and optimized the speed of the UAV to improve channel access probability.

These studies show that speed control is an effective means of solving problems caused by the distribution density of terrestrial network nodes, but the issue of communication unfairness caused by the density of UEs on the ground remains unresolved. Therefore, the objective of this study is to devise a speed-control technique for UAVs that focuses on the fairness of transmitted data for each UE.

III. SYSTEM MODEL

This section is divided into two subsections: the first one explains our system model and specifies the parameters for the UAV and UEs, while the second one covers how we mathematically express the potential amount of data transmitted by each UE based on the geographical relationship between them and the UAV, culminating in the objective function used in this study. To make it easier to follow the mathematics in this paper, all symbols used are listed in Table 1.

A. MODEL OF THE CIRCLING UAV

As shown in Fig. 1, we use a UAV-aided information collection system, where a single UAV is employed as a flying base station to collect information from K_{tot} ground-based UEs. We use cylindrical coordinates, and the k-th UE is assumed

TABLE 1. List of symbols used throughout this paper.

Notations	Description
K_{tot}	The number of UEs in the service area.
M	The number of time slots that meet the control interval of the angular velocity.
N	Total number of time slots.
r_{UE_k}	Radius of the k-th UE.
r_{UAV}	Radius of the UAV.
θ_{UE_k}	Angle of the k-th UE.
θ_{UAV}	Angle of the UAV.
H_{UAV}	Height of the UAV.
$K(\theta)$	The number of UEs that the UAV accommodates at a turn angle θ.
R	Radius of the service area.
T	Turn period of the UAV.
B	The amount of bandwidth the UAV can allocate.
p_{UE_k}	Transmit power of the UEs.
$\omega(t_n)$	Angular velocity of the UAV for the time between t_n and t_{n+1}.
δ_t	Length of the bandwidth allocation time frame.
δ_ω	Length of the speed control time frame.
l_k	Distance between the UAV and the k-th UE.
$g_k(t_n)$	Channel gain of the k-th UE at the n-th time frame.
γ_k	SNR of the k-th UE.
r_k	Transmission rate of the k-th UE.
N_0	Spectral density of the additive white Gaussian noise at the UAV.
d_k	The amount of data transmitted by the k-th UE when the UAV makes one round of its trajectory.
N_k^S	The sequential number of the time frame when the k-th UE starts to transmit to the UAV.
N_k^E	The sequential number of the last time frame the k-th UE transmits to the UAV.
θ_k	Size of the range of the UAV's turn angle in which the k-th UE can transmit to it.
$\omega_{\min}$	Minimum speed of the UAV.
$\omega_{\max}$	Maximum speed of the UAV.
$\omega_\theta(\theta_n)$	Angular velocity of the UAV for the turn angle between θ_n and θ_{n+1}.
$t_u(\theta_n)$	Flight time from θ_n to θ_{n+1}.
$t(\theta_n)$	Total flight time up to angle θ_n.
$(N_k^S)^*$	The sequential number for the turn angle at which the k-th UE begins transmitting to the UAV.
$(N_k^E)^*$	The sequential number for the last turn angle at which the k-th UE transmits to the UAV.

to exist at a fixed location given by $(r_{UE_k}, \theta_{UE_k}, 0)$. The UAV flies in the $+\theta$ direction at a fixed radius r_{UAV} and altitude H_{UAV}, with a turn period of T. Its position is expressed as $(r_{UAV}, \theta_{UAV}, H_{UAV})$. The service area covered by the flying UAV is a circle with radius $R = 2r_{UAV}$. The number of UEs that the UAV accommodates at a turn angle θ is denoted as $K(\theta)$. The UAV knows the position of the UEs in advance from its previous passage along the flight trajectory.

The bandwidth allocation is calculated at discretized points in time and denoted by $t_n, n \in \{0, 1, \ldots, N\}$, with $t_N = T$. The length of each time frame is represented by δ_t. The UAV and UEs are connected by adopting Orthogonal Frequency Division Multiple Access (OFDMA), and the amount of bandwidth the UAV can allocate is denoted by B. In this system, bandwidth is allocated equally to UEs in the UAV coverage area.

Since the UAV's trajectory has a fixed radius, we use the angular velocity instead of the speed. The angular velocity of the UAV at a time between t_n and t_{n+1} is given by $\omega(t_n)$, and

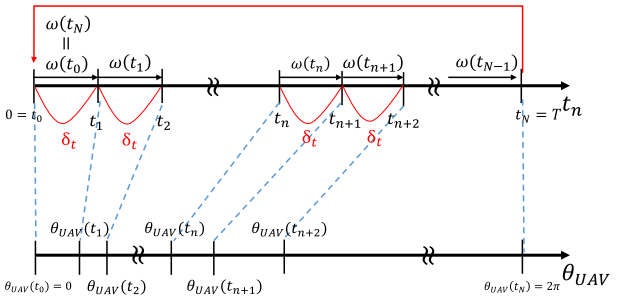

FIGURE 2. Relationship between $\omega(t_n)$ and $\theta_{UAV}(t_n)$.

the control interval of the angular velocity is denoted by δ_ω, with $\delta_t < \delta_\omega$. With these variables defined, we can formulate the following equation.

$$\omega(t_k) = \omega(t_{k+1}) = \ldots = \omega(t_{k+M-1}) \quad (k = Mk'(k' = 0, 1, 2, \ldots)), \tag{1}$$

where $M = \delta_\omega/\delta_t$ is the number of slots that meet the control interval of the angular velocity δ_ω. There is also a relationship between the angular velocity of a UAV and its turn angle given by

$$\theta_{UAV}(t_n) = \begin{cases} 0, & n = 0 \\ \delta_t \sum_{i=0}^{n-1} \omega(t_i), & n \geq 1. \end{cases} \tag{2}$$

The relationship between the angular velocity of the UAV at time t_n, $\omega(t_n)$, and its turn angle at time t_n, $\theta_{UAV}(t_n)$, is illustrated in Fig. 2.

The distance between the UAV and the k-th UE in the n-th time frame is calculated using the Law of Cosines:

$$l_k(t_n) = \{{r_{UE_k}}^2 + {r_{UAV}}^2 + {H_{UAV}}^2 - 2 r_{UE_k} r_{UAV} \cos(\theta_{UE_k} - \theta_{UAV}(t_n))\}^{\frac{1}{2}}. \tag{3}$$

B. FORMULATION OF THE AMOUNT OF TRANSMITTED DATA

In this subsection, we present a formulation for quantifying communication fairness. Prior studies have measured fairness in terms of the throughput of each UE [35], [36], but this metric is not appropriate for our model because no UE is always in the UAV's coverage area. Therefore, in this paper, communication fairness is determined from the amount of data transmitted by a UE when the UAV makes one round of its trajectory.

[15] showed that the LoS probability increases as the altitude of the UAV increases, and that the LoS probability is more than 95% for a UAV at 120 m. Thus, for simplicity, we use the free-space pass loss model as the propagation model: the channel gain of the k-th UE at the n-th time frame, $g_k(t_n)$, is assumed to depend primarily on the distance and can be expressed as

$$g_k(t_n) = \left(\frac{\lambda}{4\pi l_k(t_n)}\right)^2, \tag{4}$$

where λ denotes the wavelength of the carrier wave.

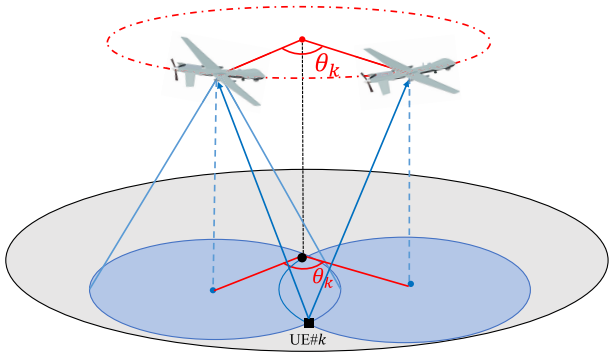

FIGURE 3. An illustration of θ_k.

Accordingly, the SNR, $\gamma_k(t_n)$, and the transmission rate, derived from the Shannon-Hartley theorem, $r_k(t_n)$, of the k-th UE in the n-th time frame can be expressed as

$$\gamma_k(t_n) = \frac{g_k(t_n) p_{UE} K(\theta_{UAV}(t_n))}{B N_0} \tag{5}$$

$$r_k(t_n) = \frac{B}{K(\theta_{UAV}(t_n))} \log_2(1 + \gamma_k(t_n)), \tag{6}$$

where p_{UE} denotes the transmit power of the UEs, and N_0 represents the spectral density of the additive white Gaussian noise at the UAV.

The amount of transmitted data for the k-th UE, d_k, is given by

$$d_k = \delta_t \sum_{n=N_k^S}^{N_k^E} r_k(t_n), \tag{7}$$

where N_k^S is the sequential number of the time frame when the k-th UE starts to transmit to the UAV and N_k^E is the sequential number of the last time frame the k-th UE transmits to the UAV.

The relationship between the time when the k-th UE transmits to the UAV and the UAV's angular velocity, illustrated in Fig. 3, is given by

$$\delta_t \sum_{n=N_k^S}^{N_k^E} \omega(t_n) = \theta_k, \tag{8}$$

where θ_k is the size of the range of the UAV's turn angle in which the k-th UE can transmit to it. θ_k is uniquely determined by r_{UE_k}.

To balance the total amount of transmittable data and fairness among the UEs, we formulate the speed control problem as follows:

$$\underset{\omega(t_n)}{\text{maximize}} \quad \min_k d_k, \tag{9a}$$

$$\text{subject to} \quad \frac{1}{N} \sum_{n=0}^{N-1} \omega(t_n) = \frac{2\pi}{T}, \tag{9b}$$

$$\omega_{\min} \leq \omega(t_n) \leq \omega_{\max}, \quad \forall n \in \{0, 1, \ldots, N\} \tag{9c}$$

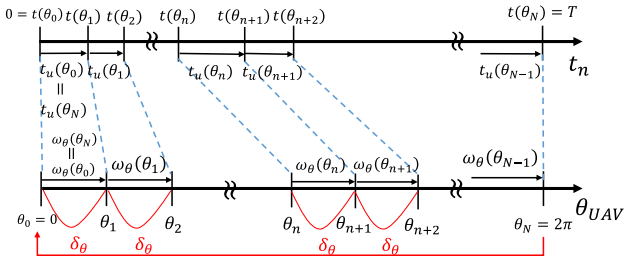

FIGURE 4. Relationship between $t(\theta_n)$ and $\omega_\theta(\theta_n)$.

(9b) specifies that the turn period of the UAV is constant, and (9c) places bounds on the speed of the UAV. Note that problem (9a) is difficult to solve because there are N optimization parameters, $\omega(t_n)$, and strict constraints, (9b) and (9c), exist. Because the speed of the UAV takes a continuous value, an exhaustive search method cannot be applied. Even with discretized velocities, the search space remains enormous, and extremely high computational complexity is unavoidable because the speeds of the UAV at all speed-control intervals need to be determined. A low-complexity algorithm is required so that the calculation can be quickly executed for each lap.

IV. PROPOSED METHOD

In this section, we elaborate on our method throughout four subsections. In the first subsection, we introduce the discretized turn angle and the UAV's angular velocity at each point of it, and we rewrite the expression for the amount of transmitted data from a UE. We then discuss the design policy for our method. In the three subsections that follow, we give a detailed overview of the three processes involved in calculating the angular velocity of the UAV. Finally, we analyze the complexity and convergence of our proposed method.

A. DESIGN POLICY

To measure the quantitative relationship between angular velocity and the amount of transmitted data, we introduce a discretized turn angle for the UAV, θ_n with $\theta_N = 2\pi$. We can use this to obtain a discretized interval of $\delta_\theta = 2\pi/N$. The angular velocity at each turn angle of the UAV is represented by $\omega_\theta(\theta_n)$. The time for the UAV to fly between θ_n and θ_{n+1}, $t_u(\theta_n)$, and the total flight time up to angle θ_n, $t(\theta_n)$, are calculated as

$$t_u(\theta_n) = \frac{\delta_\theta}{\omega_\theta(\theta_n)} \tag{10}$$

$$t(\theta_n) = \begin{cases} 0, & n = 0 \\ \delta_\theta \sum_{i=0}^{n-1} \frac{1}{\omega_\theta(\theta_i)}, & n \geq 1. \end{cases} \tag{11}$$

The relationship between θ_n and $t(\theta_n)$ is illustrated in Fig. 4. Therefore, we redefine (3), (4), (5), and (6) as

$$l_k(\theta_n) = \{{r_{UE_k}}^2 + {r_{UAV}}^2 + {H_{UAV}}^2 - 2 r_{UE_k} r_{UAV} \cos(\theta_{UE_k} - \theta_n)\}^{\frac{1}{2}} \tag{12}$$

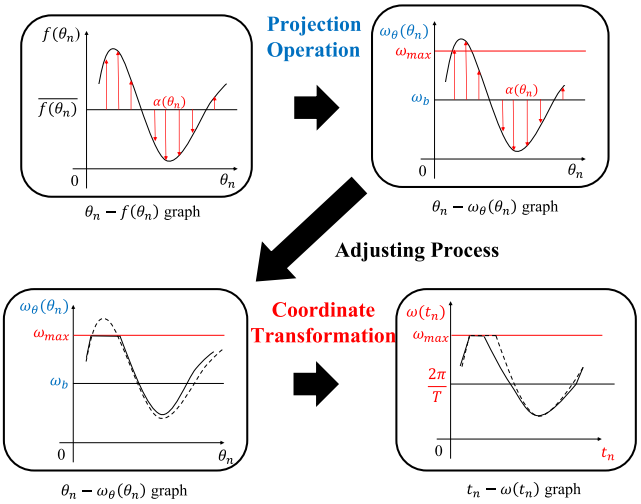

FIGURE 5. Operation workflow.

$$g_k(\theta_n) = \left(\frac{\lambda}{4\pi l_k(\theta_n)}\right)^2 \tag{13}$$

$$\gamma_k(\theta_n) = \frac{g_k(\theta_n) p_{UE} K(\theta_n)}{B N_0} \tag{14}$$

$$r_k(\theta_n) = \frac{B}{K(\theta_n)} \log_2(1 + \gamma_k(\theta_n)). \tag{15}$$

Hence, the amount of transmitted data for the k-th UE is expressed as

$$\begin{aligned} d_k &= \sum_{n=(N_k^S)^*}^{(N_k^E)^*} r_k(\theta_n) t_u(\theta_n) \\ &= B\delta_\theta \sum_{n=(N_k^S)^*}^{(N_k^E)^*} \frac{\log_2(1 + \gamma_k(\theta_n))}{K(\theta_n)\omega_\theta(\theta_n)}, \end{aligned} \tag{16}$$

where $(N_k^S)^*$ is the sequential number for the turn angle at which the k-th UE begins transmitting to the UAV, and $(N_k^E)^*$ is the sequential number for the last turn angle at which it does so.

In this paper, we focus on unfairness in the ability of UEs to transmit data caused by an uneven spatial distribution of its users. Therefore, we make two assumptions for simplicity. One is that the size of the communication range is a constant value $(N^R)^*$ for all UEs. The other is that the frequency utilization efficiency for each UE is equal to the average of that at each turn angle. Given these two assumptions, the amount of data transmitted by each UE depends only on $(N_k^S)^*$, and (16) can be rewritten as

$$d_k = B\delta_\theta \sum_{n=(N_k^S)^*}^{(N_k^S)^*+(N^R)^*} \frac{\overline{\log_2(1 + \gamma_k(\theta_n))}}{K(\theta_n)\omega_\theta(\theta_n)}. \tag{17}$$

We denote the functions $f(\theta_n)$, $r(\theta_n)$, and $d(\theta_n)$ as

$$f(\theta_n) = \frac{\overline{\log_2(1 + \gamma_k(\theta_n))}}{K(\theta_n)} \tag{18}$$

$$r(\theta_n) = Bf(\theta_n) \tag{19}$$
$$d(\theta_n) = r(\theta_n)t_u(\theta_n), \tag{20}$$

where $r(\theta_n)$ is the average transmitted data rate for UEs at each turn angle. $d(\theta_n)$ represents the average amount of data transmitted by UEs when the UAV flies between θ_n and $(\theta_n + \delta_\theta)$, and is henceforth referred to as the micro-amount of transmitted data. Additionally, the function $I(\theta_n)$ is defined as

$$I(\theta_n) = \frac{f(\theta_n)}{\omega_\theta(\theta_n)}. \tag{21}$$

Applying this to (17) gives

$$d_k = B\delta_\theta \sum_{n=(N_k^S)^*}^{(N_k^S)^*+(N^R)^*} I(\theta_n). \tag{22}$$

Therefore, if $I(\theta_n)$ is always constant, independent of θ_n, then the amount of data transmitted is constant regardless of $(N_k^S)^*$, and under these assumptions, the amount of data transmitted becomes equal among UEs. Hence, to ensure fairness in the amount of data transmitted by each UE, we have to derive an angular velocity $\omega_\theta(\theta_n)$ that makes $I(\theta_n)$ constant. This is the design policy for our method.

In the following subsections, we calculate the angular velocity of the UAV in three steps: Projection Operation, Adjusting Process, and Coordinate Transformation. In Projection Operation, we calculate $\omega_\theta(\theta_n)$ to satisfy (9b) by referencing the value of $f(\theta_n)$. The Adjusting Process involves adjusting the angular velocity until it satisfies (9c). Finally, Coordinate Transformation involves transforming $\omega_\theta(\theta_n)$ into $\omega(t_n)$. The workflow for these three steps is shown in Fig. 5.

B. PROJECTION OPERATION

In this operation, we calculate the angular velocity at each turn angle $\omega_\theta(\theta_n)$ while only considering constraints to the turn period T.

We begin by defining a constant $\alpha(\theta_n)$ as

$$\alpha(\theta_n) = \frac{f(\theta_n)}{\overline{f(\theta_n)}} = \frac{\omega_\theta(\theta_n)}{\omega_b}, \tag{23}$$

where ω_b is the base angular velocity, which is constant. By defining $\alpha(\theta_n)$ in this way, (21) can be rewritten as

$$I(\theta_n) = \frac{\alpha(\theta_n)\overline{f(\theta_n)}}{\alpha(\theta_n)\omega_b} = \frac{\overline{f(\theta_n)}}{\omega_b}. \tag{24}$$

Therefore, $I(\theta_n)$ becomes constant regardless of θ_n, thereby satisfying the design principles for our method.

Next, we have to determine the base angular velocity ω_b. Using (11) we obtain

$$T = \delta_\theta \sum_{n=0}^{N-1} \frac{1}{\omega_\theta(\theta_n)} = 2\pi\overline{\left(\frac{1}{\omega_\theta(\theta_n)}\right)}. \tag{25}$$

Additionally, deforming (25) using (23), ω_b can be written as

$$\omega_b = \frac{2\pi}{T}\overline{\left(\frac{1}{\alpha(\theta_n)}\right)}. \tag{26}$$

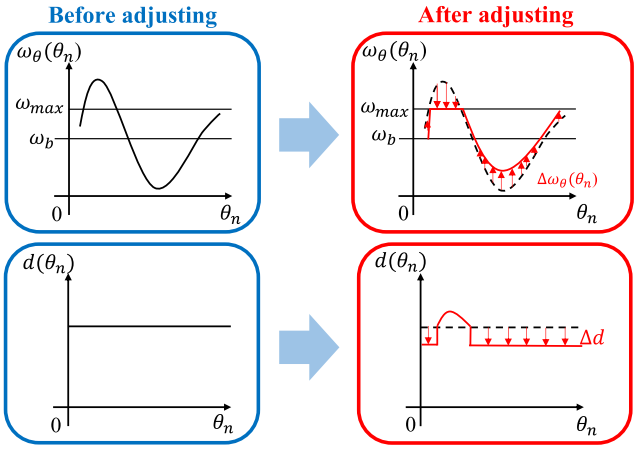

FIGURE 6. Explanation of the adjusting process.

Finally, the angular velocity $\omega_\theta(\theta_n)$ can be obtained from (23).

C. ADJUSTING PROCESS

The angular velocity $\omega_\theta(\theta_n)$ is obtained from the Projection Operation, but it does not always satisfy the speed limit of the UAV. If this is the case, then the Adjusting Process needs to be conducted. The Adjusting Process calculates a kind of compromise solution that satisfies the speed limit of the angular velocity based on the angular velocity obtained by the Projection Operation. The Adjusting Process can be divided into two main operations. The first is changing the angular velocity component so that it lies within the bounds set by $\omega_{\min}$ and $\omega_{\max}$. The second is to adjust the angular velocity so that it satisfies the following two conditions: the turn period of the UAV does not change before and after the Adjusting Process, and the change in the amount of micro-transmitted data at each turn angle due to this operation, Δd, is a constant independent of the turn angle. The change in angular velocity satisfying these two conditions, $\Delta\omega_\theta(\theta_n)$, can be easily obtained, and the reduction in fairness due to speed limits can be decreased. The changes in the angular velocity and the amount of micro-transmitted data due to these operations are illustrated in Fig. 6.

Henceforth, we will denote the set of turn angles in which the angular velocity $\omega_\theta(\theta_n)$ does not meet the speed limit before the Adjusting Process as $\mathcal{O}$, and conversely, the set of turn angles in which it does as $\mathcal{L}$. First, if the angular velocity is over the speed limit, then it is restored to the speed limit. Second, the effect of this correction on the turn period is calculated. We begin doing so by looking at the change in $t_u(\theta_n)$ when the angular velocity changes from $\omega_\theta(\theta_n)$ to $(\omega_\theta(\theta_n) + \Delta\omega_\theta(\theta_n))$, which is given by

$$\begin{aligned}\Delta t_u(\theta_n) &= \frac{\delta_\theta}{\omega_\theta(\theta_n) + \Delta\omega_\theta(\theta_n)} - \frac{\delta_\theta}{\omega_\theta(\theta_n)} \\ &= t_u(\theta_n)\left(-\frac{\Delta\omega_\theta(\theta_n)}{\omega_\theta(\theta_n) + \Delta\omega_\theta(\theta_n)}\right).\end{aligned} \tag{27}$$

Algorithm 1 :Transformation Algorithm

Input: ω_θ
Output: ω

1: **for** $n = 0 \ldots N-1$ **do**
2: **if** $n = 0$ **then**
3: $\omega(t_n) \Leftarrow \omega_\theta(\theta_n)$
4: **else**
5: $\theta_{UAV}(t_n) \Leftarrow \theta_{UAV}(t_{n-1}) + \delta_t \times \omega(t_{n-1})$
6: $a \Leftarrow \lfloor \theta_{UAV}(t_n)/\delta_\theta \rfloor$
7: $r \Leftarrow \theta_{UAV}(t_n)/\delta_\theta - a$
8: **if** $a \geq N$ **then**
9: $\omega(t_n) \Leftarrow \omega_{\min}$
10: **else**
11: $g \Leftarrow \omega_\theta(\theta_{a+1}) - \omega_\theta(\theta_a)$
12: $\omega(t_n) \Leftarrow \omega_\theta(\theta_a) + g \times r$
13: **end if**
14: **end if**
15: **end for**

Then, the change in the UAV's flight time from restoring the angular velocity to the speed limit is calculated as

$$t_o = \sum_{\theta_n \in \mathcal{O}} \Delta t_u(\theta_n). \tag{28}$$

After that, we adjust the angular velocity, which now meets the speed limit, so that it satisfies two additional conditions. The first is that the turn period after the speed change is equal to that before the speed change. This condition is expressed as

$$t_o + \sum_{\theta_n \in \mathcal{L}} \Delta t_u(\theta_n) = 0. \tag{29}$$

The other is that the change in the data once this change is made, Δd, is constant for $\theta_n \in \mathcal{L}$. Using (20), we can write this as

$$\Delta d = r(\theta_n)\Delta t_u(\theta_n) \quad \forall \theta_n \in \mathcal{L}. \tag{30}$$

Using (29) and (30), Δd can be uniquely obtained as

$$\Delta d = -t_o \left(\sum_{\theta_n \in \mathcal{L}} \frac{1}{r(\theta_n)} \right)^{-1}. \tag{31}$$

Also, using (20), (27), and (30), $\Delta\omega_\theta(\theta_n)$ can be calculated as

$$\Delta\omega_\theta(\theta_n) = -\frac{\Delta d}{d(\theta_n) + \Delta d}\omega_\theta(\theta_n) \quad \forall \theta_n \in \mathcal{L}. \tag{32}$$

This can then be added to the original angular velocity to obtain the angular velocity after the change. Since changing the angular velocity values in a set $\mathcal{L}$ may result in values that do not satisfy the speed limit, the Adjusting Process is continued until all components of the angular velocity do satisfy it.

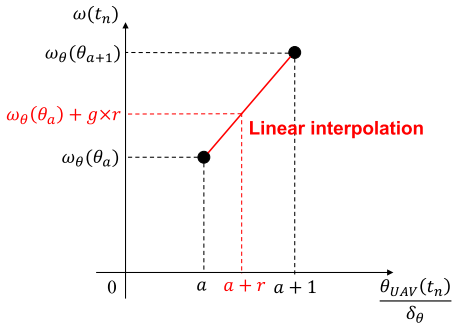

FIGURE 7. Linear interpolation.

Algorithm 2 :Averaging Algorithm

Input: ω (Before averaging)
Output: ω (After averaging)

1: $\omega_{\text{sum}} \Leftarrow 0$
2: **for** $n = 0 \ldots N-1$ **do**
3: $\omega_{\text{sum}} \Leftarrow \omega_{\text{sum}} + \omega(t_n)$
4: **if** $(n+1) \bmod M = 0$ **then**
5: **for** $m = 1 \ldots M$ **do**
6: $\omega(t_{n+m-M}) \Leftarrow \omega_{\text{sum}}/M$
7: **end for**
8: $\omega_{\text{sum}} \Leftarrow 0$
9: **end if**
10: **end for**

D. COORDINATE TRANSFORMATION

Consider (2) and (11). We translate the angular velocity at each turn angle, $\omega_\theta(\theta_n)$, so that they equal those in the bandwidth allocation time $\omega(t_n)$ of Algorithm 1. Lines 2 and 3 mean $\omega(t_0) = \omega_\theta(\theta_0) = \omega_\theta(\theta_N)$. This is because the angular velocity when the UAV starts turning is equal to that when it finishes turning, as illustrated in Fig. 2 and Fig. 4. The current turn angle of the UAV is calculated in line 5. We then compute the angular velocity corresponding to it. However, the discontinuous angular velocity at each turn angle creates a problem: if the current turn angle is between two discretized turn angles, then the angular velocity corresponding to it does not exist. To solve this problem, we use linear interpolation. Linear interpolation is a method for connecting discrete values with a straight line, assuming that the values between them share a linear relationship. First, divide the current turn angle by the slot width δ_θ and extract the integer part a and the decimal part r, which is done in lines 6 and 7. Second, take the difference between $\omega_\theta(\theta_a)$ and $\omega_\theta(\theta_{a+1})$. This is the grand of the angular velocity in unit slots. By multiplying this grand g by the decimal part r and adding the velocity in slot a, the angular velocity corresponding to the current position can be derived. This series of calculations is illustrated in Fig. 7. The operation in line 9 indicates that if the turn angle exceeds 2π, the angular velocity is assigned $\omega_{\min}$. These operations are continued until the angular velocities at all times are obtained. However, linear interpolation causes a minute error, and the

TABLE 2. Computational complexity of each process.

Process	Computational complexity
Projection Operation	$\mathcal{O}(NK_{tot})$
Adjusting Process	$\mathcal{O}(N)$
Coordinate Transformation	$\mathcal{O}(NM)$
Total	$\mathcal{O}(NK_{tot}+NM)$

angular velocity of the UAV does not satisfy (9b). Therefore, the derived angular velocity needs to be finely arranged to satisfy the limit (9b). The algorithm for this can be found in the Appendix.

As the angular velocity varies with each frame length δ_t, we use Algorithm 2 to take the average value for each interval to meet the velocity control interval δ_ω. First, ω_{sum} is initialized in line 1. Then, in line 3, the sum of each of the M slots is stored in ω_{sum}, which is then averaged and assigned to ω in line 6. ω_{sum} is then initialized in line 8. Coordinate Transformation is performed using these algorithms until the desired angular velocity is finally obtained.

E. ANALYSIS OF COMPLEXITY AND CONVERGENCE

In this subsection, we analyze the computational complexity and the convergence of the proposed method. Table 2 summarizes the computational complexity of each process in the proposed method. The Projection Operation requires $f(\theta_n)$ in (23), which is obtained from (18). To obtain the numerator of (18) in a certain slot, γ_k of each of the K_{tot} UEs needs to be calculated. Therefore, the Projection Operation requires $f(\theta_n)$ for N slots, so the computational complexity is $\mathcal{O}(NK_{tot})$. The Adjusting Process involves calculations using formulas (27) to (32). The computational complexity for each formula is at most $\mathcal{O}(N)$, so the computational complexity of the Adjusting Process is also $\mathcal{O}(N)$. The Coordinate Transformation consists of Algorithm 1, Algorithm 2, and Algorithm 3. Algorithm 2 has the most computational complexity, totaling $\mathcal{O}(NM)$, so the computational complexity of the Coordinate Transformation is also $\mathcal{O}(NM)$. Therefore, the total computational complexity of the proposed method is $\mathcal{O}(NK_{tot}+NM)$.

To assess the efficiency of the proposed method, we compare its computational complexity to that of the Brute Force method. In the Brute Force method, P patterns of speed sets are prepared, and the speed of the UAV is determined by trying them all. The computational complexity is $\mathcal{O}(NK_{tot}P)$ because the amount of data transmitted by K_{tot} UEs in N time frames needs to be calculated P times. The number of patterns P is determined by the number of levels of UAV speed L and the speed control interval $\delta_\omega = M\delta_t$, where $P = L^{\frac{T}{\delta_\omega}}$. Therefore, the computational complexity is $\mathcal{O}(NK_{tot}L^{\frac{T}{\delta_\omega}})$, and this is not a calculable quantity. Thus, it is clear that our method for calculating UAV velocity requires a much lower computational cost than the Brute Force method.

Next, we confirm the convergence of the proposed method. In the Adjusting Process, the calculation of (10) to (32) is continued until all components of the angular velocity satisfy it. Suppose that t_o is positive in (28). In this case, the speed of the set $\mathcal{L}$ is increased so as to satisfy the condition on the turn period. If no new velocity component exceeding the upper limit appears, then the Adjusting Process converges. If new velocity components exceeding the upper limit do appear, then after first lowering them to the upper limit and placing them in the set $\mathcal{O}$, the speed of the set $\mathcal{L}$ needs to be increased again. In this way, the speed of the set $\mathcal{L}$ continues to increase. The amount of speed exceedance decreases as the Adjusting Process is repeated, and it will eventually converge because the upper speed limit is set greater than the average speed. The same is true when t_o is negative. Therefore, the Adjusting Process always converges. In the Coordinate Transformation, it is obvious that Algorithm 1 and Algorithm 2 converge, and Algorithm 3 also converges as described in the Appendix. Thus, it can be seen that the proposed method converges.

TABLE 3. Parameter settings.

Parameter	Value
B	20 MHz
K_{tot}	100, 200, 300
f	2 GHz
p_{UE}	10 mW
δ_t	10 ms
N_0	4.14×10^{-21} W/Hz
H_{UAV}	100 m
r_{UAV}	65.2 m
T	60 s
$\omega_{\min}$	$1/r_{UAV}$ rad/s
$\omega_{\max}$	$20/r_{UAV}$ rad/s
δ_ω	1 s

V. PERFORMANCE EVALUATION

In this section, we present the results of a MATLAB simulation and evaluate the performance of our speed-control technique.

A. SIMULATION SETTINGS

In this subsection, we give an overview of our simulation settings, the distribution model for UEs, and the comparative method. The simulation parameters listed in Table 3 were set by referring to the configuration of 5G base stations [37]. The maximum speed of the UAV is set to the upper value at which the flying UAV can maintain a connection with ground-based UEs [34]. It is carried out on the distribution model for UEs shown in Fig. 8. In this model, the circle is divided into four areas: a dense area, a sparse area, and two normal areas. The dense area and the sparse area are one fourth the size of the whole area. Half of the UEs are located in the dense area and 10% in the sparse area. The rest is located in the normal areas. The UEs are scattered in the range of $0 < r_{UE_k} < 0.9R$.

We use the following three speed-control techniques for performance comparison.

- **Constant**- An algorithm maintains a constant speed for the UAV with a turn period T,

$$\omega(t_n) = \frac{2\pi}{T}. \tag{33}$$

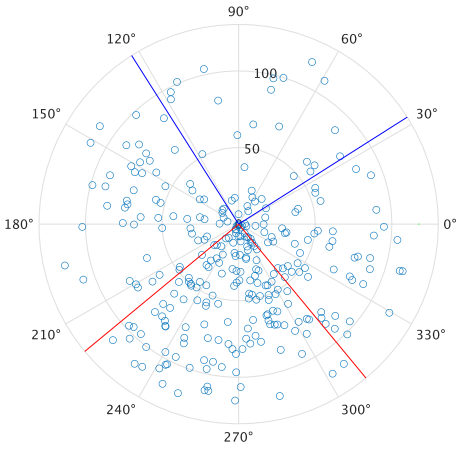

FIGURE 8. Example of a distribution model of UEs.

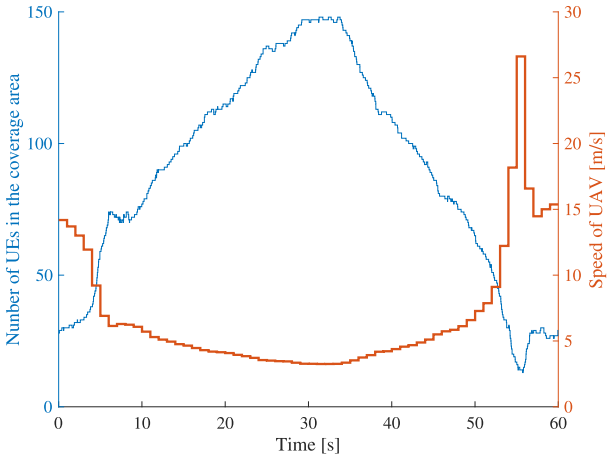

FIGURE 9. Change in the number of UEs accommodated and the speed of the UAV at each time.

- **Brute Force**- An algorithm simulates all the prepared speed patterns and uses the one that satisfies T and achieves the highest minimum amount of transmitted data. To keep the computational complexity down to a computable level, we set the speed of the UAV using the following equation and the speed control interval $\delta_\omega = 10$ s. Nevertheless, this method still has a high computational complexity and cannot be used in real-time.

$$\omega(t_n) = \frac{2\pi}{T} + \frac{\Delta V}{R} \quad (\Delta V = \{-6, -3, 0, 3, 6, 9\}). \tag{34}$$

- **Proposed**- Using our method.

First, we compare these three techniques to confirm the effectiveness of speed control in a scenario without constraint (9c), which means $\omega_{\min} = 0$ and $\omega_{\max} = \infty$. Then, we investigate whether our technique satisfies (9b) and (9c), and we demonstrate its performance.

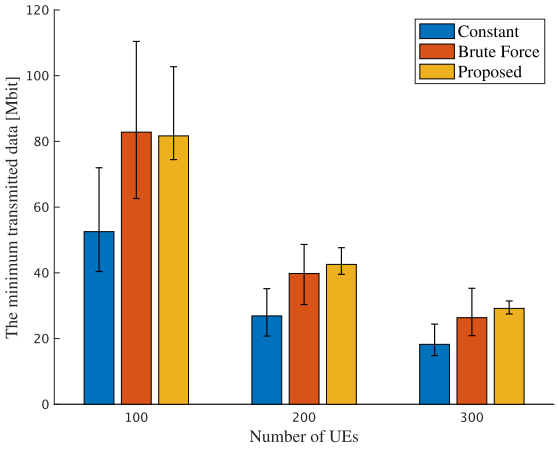

FIGURE 10. Minimum amount of transmitted data without the speed limit.

B. PERFORMANCE WITHOUT SPEED LIMIT

In this subsection, we demonstrate how our method performs without the speed limit. First, we use a simulation to confirm how the speed of the UAV changes. Fig. 9 shows the change in the number of UEs accommodated and the speed of the UAV at each time. It can be seen that the UAV adjusts its speed in response to the distribution density of users on the ground, slowing down when it is higher and speeding up when it is lower.

Next, we show the impact of each method on the amount of data transmitted by UEs. First, Figure 10 shows the minimum amount of transmitted data for each method at different values for the total number of UEs, $K_{tot} = \{100, 200, 300\}$. The simulation was conducted 1000 times. We can confirm that our method for controlling the speed of the UAV resulted in improved performance compared with that of Constant. Moreover, our method has comparable performance in terms of mean values and superior minimum values compared with that of Brute Force, which has a high computational complexity.

Then, we identify the effectiveness of the amount of data transmitted over all UEs for each method. Figure 11 gives Jain's fairness index [38] for each method, and Table 4 shows the average and the variance of the amount of transmitted data. These simulations were also conducted 1000 times. We find that, compared with other methods, our method makes the fairness index increase and the variance decrease while maintaining the average amount of transmitted data. This means our method achieves high fairness in the amount of data transmitted by UEs.

These results show that our method raises the amount of data transmitted by the UEs, which was lower when the UAV travelled at constant speed, and improves fairness. This is because our proposed method determines the speed of the UAV at which equation (21) is constant. When (21) is constant, the amount of data transmitted by each UE is also constant, even given the unfairness from the distribution

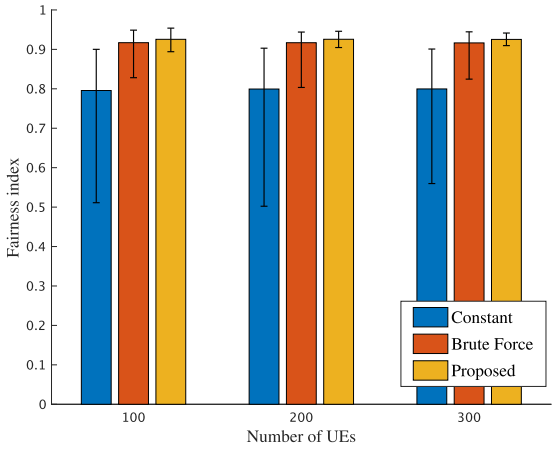

FIGURE 11. Fairness index for transmitted data without the speed limit.

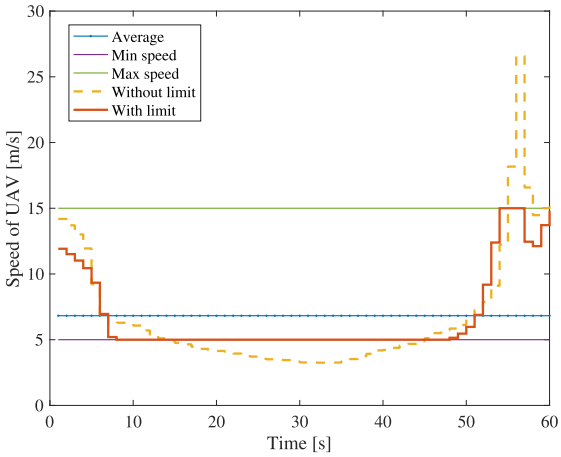

FIGURE 12. Snapshot of the angular velocity of the UAV.

TABLE 4. Average amount of transmitted data and the variance of transmitted data without speed limit.

Method \ K_{tot}	Average [Mbit]			Variance [Mbit^2]		
	100	200	300	100	200	300
Constant	184	98.1	67.8	8987	2482	1177
Brute Force	188	100	69.1	3250	915.0	437.4
Proposed	188	100	69.1	2890	811.2	387.5

TABLE 5. Minimum and maximum speed of the UAV for 3000 trials.

Speed [m/s]	Limit	Proposed
Min	1.00	3.29
Max	20.0	20.0

density of the UEs. In other words, our method adjusts the speed of the UAV according to changes in the number of UEs in the coverage area and resolves the unfairness caused by an uneven spatial distribution of UEs.

C. PERFORMANCE WITH SPEED LIMIT

We begin this subsection by presenting the change in the speed of the UAV when the Adjusting Process is conducted, which confirms that the speed control works within the speed limit. We next confirm that it satisfies (9b) and (9c). Finally, simulation results confirm the effectiveness of our method when under the speed limit.

The speed of the UAV is first compared between two trials, one with the speed limit and one without it. This was done to ensure that our method does in fact maintain the speed within the speed limit, but it was also done to see how the speed changed when speed limits were imposed. Fig. 12 shows how the speed of the UAV changed when the Adjusting Process was conducted. In this trial, we set the speed limit as $V_{\min} = r_{UAV}\omega_{\min} = 5$ m/s and $V_{\max} = r_{UAV}\omega_{\max} = 15$ m/s. We found that the Adjusting Process ensures that the angular velocity adheres to the speed limit. Moreover, even if speed limits are imposed, the positive and negative speeds relative to the average speed do not change, so the characteristics of the speed change remain.

Table 5 presents the minimum and maximum speeds of the UAV. These were obtained using the angular velocities from 1000 trials for each of the cases where $K_{tot} = 100, 200, 300$. This table indicates that the Adjusting Process and the Coordinate Transformation satisfy (9c). Moreover, the minimum and maximum turn angles of the UAV, $\theta_{UAV}(T)$, were 6.2832, which indicates that (9b) was satisfied.

We then show the impact of each method on the amount of data transmitted by UEs. Figure 13 gives the minimum amount of transmitted data for each method with varying numbers of UEs, and it shows that our model is an improvement over Constant. Moreover, our method performed as well as Brute Force in terms of the mean value, and better in terms of the minimum value. This is the same as when there is no speed limit, which indicates that our method still maintains the performance even with the speed limit.

Moreover, we assess how effective each method is in transmitting data over all UEs. Figure 14 gives the Jain's fairness index [38] for each method, and Table 6 shows the average and the variance of the amount of transmitted data. We find that, compared with the other methods, our method makes the fairness index increase and the variance decrease while maintaining the average amount of transmitted data. This means our method achieves high fairness in the amount of data transmitted by UEs.

These results indicate that the Adjusting Process maintains the performance of the proposed method. This is because the relative speed, large and small, according to the distribution density of UEs is kept within the speed limit, as demonstrated in Fig. 12. Moreover, Fig. 13 indicates that the proposed method performs better than Brute Force as the number of UEs increase. As the number of UEs increases, the solution space also expands, and it becomes more difficult to obtain an optimal solution by Brute Force. On the other hand, the

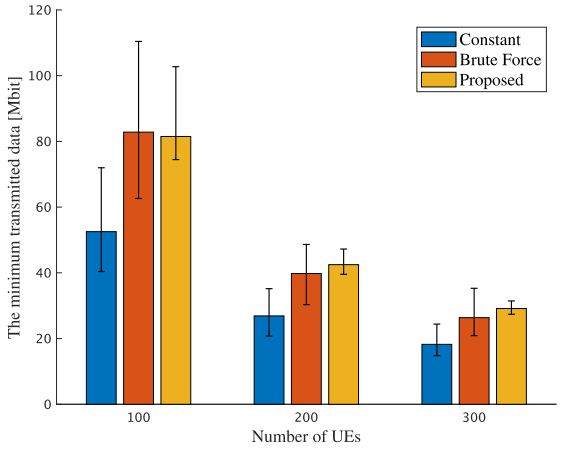

FIGURE 13. Minimum amount of transmitted data with the speed limit.

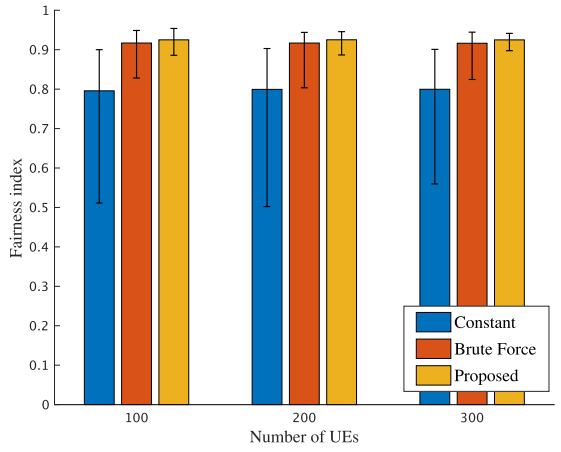

FIGURE 14. Fairness index for transmitted data with the speed limit.

TABLE 6. Average amount of transmitted data and the variance of transmitted data with the speed limit.

Method \ K_{tot}	Average [Mbit]			Variance [Mbit^2]		
	100	200	300	100	200	300
Constant	184	98.1	67.8	8987	2482	1177
Brute Force	188	100	69.1	3250	915.1	437.5
Proposed	188	100	69.1	2907	816.5	389.4

proposed method uniquely derives the speed of the UAV, so performance is independent of the number of UEs.

VI. CONCLUSION

In this paper, we have provided an overview of a new speed-control technique that uses a UAV as an aerial base station and that resolves the unfairness in communication caused by sparsely distributed users on the ground. We specifically looked at scenarios where the UAV flies in a circular trajectory above a disaster area. Through quantitative analysis of the amount of transmitted data, we developed an algorithm for deriving the angular velocity. The simulation results showed that our method increases both the minimum amount of transmitted data and fairness in the ability of UEs to communicate with the UAV. In the future, we will study the technique for achieving much fairer communications by jointly controlling the UAV's flying speed with other parameters, e.g., the bandwidth allocated to each UE.

Algorithm 3 Error-Correction Algorithm

Input: ω (Before correcting)
Output: ω (After correcting)

$N_{\max} \Leftarrow 0$
$N_{\min} \Leftarrow 0$
for $n = 0 \ldots N-1$ **do**
  if $\omega(t_n) = \omega_{\max}$ **then**
    $Idx_{\max}(n) \Leftarrow 1$
    $Idx_{\min}(n) \Leftarrow 0$
    $N_{\max} \Leftarrow N_{\max} + 1$
  else if $\omega(t_n) = \omega_{\min}$ **then**
    $Idx_{\max}(n) \Leftarrow 0$
    $Idx_{\min}(n) \Leftarrow 1$
    $N_{\min} \Leftarrow N_{\min} + 1$
  else
    $Idx_{\max}(n) \Leftarrow 0$
    $Idx_{\min}(n) \Leftarrow 0$
  end if
end for
$\omega_{\text{before}} \Leftarrow \omega$
while $\frac{2\pi}{T} \neq \overline{\omega}$ **do**
  $\omega \Leftarrow \omega_{\text{before}}$
  $err \Leftarrow 2\pi/T - \overline{\omega}$
  if $err > 0$ **then**
    for $n = 0 \ldots N-1$ **do**
      if $Idx_{\max}(n) = 0$ **then**
        $\omega(t_n) \Leftarrow \omega(t_n) + err \times (N/(N - N_{\max}))$
        if $\omega(t_n) \geq \omega_{\max}$ **then**
          $\omega(t_n) \Leftarrow \omega_{\max}$
          $\omega_{\text{before}}(t_n) \Leftarrow \omega_{\max}$
          $Idx_{\max}(n) \Leftarrow 1$
        end if
      end if
    end for
  else if $err < 0$ **then**
    for $n = 0 \ldots N-1$ **do**
      if $Idx_{\min}(n) = 0$ **then**
        $\omega(t_n) \Leftarrow \omega(t_n) + err \times (N/(N - N_{\min}))$
        if $\omega(t_n) \leq \omega_{\min}$ **then**
          $\omega(t_n) \Leftarrow \omega_{\min}$
          $\omega_{\text{before}}(t_n) \Leftarrow \omega_{\min}$
          $Idx_{\min}(n) \Leftarrow 1$
        end if
      end if
    end for
  end if
end while

APPENDIX
ERROR-CORRECTION ALGORITHM

This Appendix describes Algorithm 3, which corrects for errors introduced by the linear completion of Algorithm 1 and ensures that (9b) is satisfied.

$Idx_{\max}$ and $Idx_{\min}$ represent the indices for which the angular velocity of the UAV is equal to the speed limit. Lines 3 to 16 are where $Idx_{\max}$ and $Idx_{\min}$ are determined. Numbers of elements equal to the maximum and minimum speed limits, $N_{\max}$ and $N_{\min}$, respectively, are also counted.

In line 17, ω_{before} stores ω before correcting for error. If the current angular velocity does not meet the cycle, then a while loop begins in line 18. ω is initialized in line 19, and the errors for the angular velocity are calculated in line 20. Then, the operation changes somewhat depending on whether err, which represents the error in the angular velocity, is positive or negative. We will explain what happens in the case when err is positive. In line 24, the same constant is added to the angular velocity at each time to satisfy the period, but it is important to note that this addition operation cannot be performed for the angular velocity when it is already at the maximum allowable value from the speed limit. So, as long as the angular velocity is not at its maximum, this operation is carried out.

In line 25, if the maximum angular velocity is exceeded by the addition operation, then the maximum angular velocity is reassigned to that angular velocity in lines 26 and 27, and $Idx_{\max}$ is updated in line 28. In this case, the condition for exiting the while loop is not met, and the operation is reperformed starting from line 18. On the other hand, if the addition operation can be performed on all non-maximum angular velocities without exceeding the maximum value, $2\pi/T = \overline{\omega}$, and the while loop can be exited. Since the error calculated in line 20 becomes smaller and smaller as the while loop is repeated, it is ensured that the while loop will be exited and Algorithm 3 will terminate. All of these steps ensure that the angular velocity satisfies (9b).

REFERENCES

[1] Y. Zeng, R. Zhang, and T. J. Lim, "Wireless communications with unmanned aerial vehicles: Opportunities and challenges," *IEEE Commun. Mag.*, vol. 54, no. 5, pp. 36–42, May 2016.

[2] M. Mozaffari, W. Saad, M. Bennis, Y.-H. Nam, and M. Debbah, "A tutorial on UAVs for wireless networks: Applications, challenges, and open problems," *IEEE Commun. Surveys Tuts.*, vol. 21, no. 3, pp. 2334–2360, 3rd Quart., 2019.

[3] S. Zeng, H. Zhang, B. Di, and L. Song, "Trajectory optimization and resource allocation for OFDMA UAV relay networks," *IEEE Trans. Wireless Commun.*, vol. 20, no. 10, pp. 6634–6647, Oct. 2021.

[4] L. Li, Q. Cheng, K. Xue, C. Yang, and Z. Han, "Downlink transmit power control in ultra-dense UAV network based on mean field game and deep reinforcement learning," *IEEE Trans. Veh. Technol.*, vol. 69, no. 12, pp. 15594–15605, Dec. 2020.

[5] Y. Zeng and R. Zhang, "Energy-efficient UAV communication with trajectory optimization," *IEEE Trans. Wireless Commun.*, vol. 16, no. 6, pp. 3747–3760, Jun. 2017.

[6] H. Zhang, L. Song, Z. Han, and H. V. Poor, "Cooperation Techniques for a cellular Internet of Unmanned Aerial Vehicles," *IEEE Wireless Commun.*, vol. 26, no. 5, pp. 167–173, Oct. 2019.

[7] J. Miao and P. Wang, "Power control for multi-UAV location-aware wireless powered communication networks," in *Proc. IEEE/CIC Int. Conf. Commun. China (ICCC Workshops)*, Aug. 2020, pp. 225–230.

[8] Q. Wu and R. Zhang, "Common throughput maximization in UAV-enabled OFDMA systems with delay consideration," *IEEE Trans. Wireless Commun.*, vol. 66, no. 12, pp. 6614–6627, Dec. 2018.

[9] J. Zhang, F. Liang, B. Li, Z. Yang, Y. Wu, and H. Zhu, "Placement optimization of caching UAV-assisted mobile relay maritime communication," *China Commun.*, vol. 17, no. 8, pp. 209–219, Aug. 2020.

[10] D.-H. Tran, S. Chatzinotas, and B. Ottersten, "Satellite- and cache-assisted UAV: A joint cache placement, resource allocation, and trajectory optimization for 6G aerial networks," *IEEE Open J. Veh. Technol.*, vol. 3, pp. 40–54, 2022.

[11] P. K. Sharma, D. Gupta, and D. I. Kim, "Outage performance of 3D mobile UAV caching for hybrid satellite-terrestrial networks," *IEEE Trans. Veh. Technol.*, vol. 70, no. 8, pp. 8280–8285, Aug. 2021.

[12] S. Gu, X. Sun, Z. Yang, T. Huang, W. Xiang, and K. Yu, "Energy-aware coded caching strategy design with resource optimization for satellite-UAV-vehicle-integrated networks," *IEEE Internet Things J.*, vol. 9, no. 8, pp. 5799–5811, Apr. 2022.

[13] Z. Jia, M. Sheng, J. Li, D. Niyato, and Z. Han, "LEO-satellite-assisted UAV: Joint trajectory and data collection for Internet of Remote Things in 6G aerial access networks," *IEEE Internet of Things J.*, vol. 8, no. 12, pp. 9814–9826, Jun. 2021.

[14] W. Wei, J. Wang, Z. Fang, J. Chen, Y. Ren, and Y. Dong, "3U: Joint design of UAV-USV-UUV networks for cooperative target hunting," *IEEE Trans. Veh. Technol.*, early access, Nov. 9, 2022, doi: 10.1109/TVT.2022.3220856.

[15] X. Lin, V. Yajnanarayana, S. D. Muruganathan, S. Gao, H. Asplund, H.-L. Maattanen, M. Bergstrom, S. Euler, and Y.-P. E. Wang, "The sky is not the limit: LTE for unmanned aerial vehicles," *IEEE Commun. Mag.*, vol. 56, no. 4, pp. 204–210, Apr. 2018.

[16] N. Zhao, W. Lu, M. Sheng, Y. Chen, J. Tang, F. R. Yu, and K.-K. Wong, "UAV-assisted emergency networks in disasters," *IEEE Wireless Commun.*, vol. 26, no. 1, pp. 45–51, Feb. 2019.

[17] S. Chowdhury, A. Emelogu, M. Marufuzzaman, S. G. Nurre, and L. Bian, "Drones for disaster response and relief operations: A continuous approximation model," *Int. J. Prod. Econ.*, vol. 188, pp. 167–184, Jun. 2017.

[18] M. Erdelj and E. Natalizio, "UAV-assisted disaster management: Applications and open issues," in *Proc. Int. Conf. Comput., Netw. Commun. (ICNC)*, Feb. 2016, pp. 1–5.

[19] M. Peer, V. A. Bohara, and A. Srivastava, "Multi-UAV placement strategy for disaster-resilient communication network," in *Proc. IEEE 92nd Veh. Technol. Conf. (VTC-Fall)*, Nov. 2020, pp. 1–7.

[20] A. Merwaday and I. Guvenc, "UAV assisted heterogeneous networks for public safety communications," in *Proc. IEEE Wireless Commun. Netw. Conf. Workshops (WCNCW)*, Mar. 2015, pp. 329–334.

[21] S. U. Rahman, G.-H. Kim, Y.-Z. Cho, and A. Khan, "Positioning of UAVs for throughput maximization in software-defined disaster area UAV communication networks," *J. Commun. Netw.*, vol. 20, no. 5, pp. 452–463, Oct. 2018.

[22] Y. Wu, X. Guan, W. Yang, and Q. Wu, "UAV swarm communication under malicious jamming: Joint trajectory and clustering design," *IEEE Wireless Commun. Lett.*, vol. 10, no. 10, pp. 2264–2268, Oct. 2021.

[23] X. Zhang and L. Duan, "Energy-saving deployment algorithms of UAV swarm for sustainable wireless coverage," *IEEE Trans. Veh. Technol.*, vol. 69, no. 9, pp. 10320–10335, Sep. 2020.

[24] Z. M. Fadlullah, D. Takaishi, H. Nishiyama, N. Kato, and R. Miura, "A dynamic trajectory control algorithm for improving the communication throughput and delay in UAV-aided networks," *IEEE Netw.*, vol. 30, no. 1, pp. 100–105, Jan./Feb. 2016.

[25] R. D. Yates, Y. Sun, D. R. Brown, S. K. Kaul, E. Modiano, and S. Ulukus, "Age of information: An introduction and survey," *IEEE J. Sel. Areas Commun.*, vol. 39, no. 5, pp. 1183–1210, May 2021.

[26] Z. Fang, J. Wang, Y. Ren, Z. Han, H. V. Poor, and L. Hanzo, "Age of information in energy harvesting aided massive multiple access networks," *IEEE J. Sel. Areas Commun.*, vol. 40, no. 5, pp. 1441–1456, May 2022.

[27] G. Tajima and H. Nishiyama, "Fairness-aware resource allocation technique for UAV-aided information collection system in a disaster," *IEICE Commun. Exp.*, vol. 11, no. 8, pp. 474–479, Aug. 2022.

[28] S. Zhang and J. Liu, "Analysis and optimization of multiple unmanned aerial vehicle-assisted communications in post-disaster areas," *IEEE Trans. Veh. Technol.*, vol. 67, no. 12, pp. 12049–12060, Dec. 2018.

[29] X. Wang, W. Feng, Y. Chen, and N. Ge, "Sum rate maximization for mobile UAV-aided Internet of Things communications system," in *Proc. IEEE 88th Veh. Technol. Conf. (VTC-Fall)*, Aug. 2018, pp. 1–5.

[30] N. H. Chu, D. T. Hoang, D. N. Nguyen, N. V. Huynh, and E. Dutkiewicz, "Fast or slow: An autonomous speed control approach for UAV-assisted IoT data collection networks," in *Proc. IEEE Wireless Commun. Netw. Conf. (WCNC)*, Mar. 2021, pp. 1–6.
[31] Q. Pan, X. Wen, Z. Lu, L. Li, and W. Jing, "Dynamic speed control of unmanned aerial vehicles for data collection under Internet of Things," *Sensors*, vol. 18, no. 11, p. 3951, Nov. 2018.
[32] J. Gong, T.-H. Chang, C. Shen, and X. Chen, "Flight time minimization of UAV for data collection over wireless sensor networks," *IEEE J. Sel. Areas Commun.*, vol. 36, no. 9, pp. 1942–1954, Sep. 2018.
[33] Y. Fu, D. Li, Q. Tang, and S. Zhou, "Joint speed and bandwidth optimized strategy of UAV-assisted data collection in post-disaster areas," in *Proc. 20th Medit. Commun. Comput. Netw. Conf. (MedComNet)*, Jun. 2022, pp. 39–42.
[34] X. Hu, D. Li, C. Gio, W. Hu, L. Zhang, and M. Zhai, "Maximum channel access probability based on post-disaster ground terminal distribution density," in *Computational Data and Social Networks*. Cham, Switzerland: Springer, Jan. 2020, pp. 164–175.
[35] B. Hu, L. Wang, S. Chen, J. Cui, and L. Chen, "An uplink throughput optimization scheme for UAV-enabled urban emergency communications," *IEEE Internet Things J.*, vol. 9, no. 6, pp. 4291–4302, Mar. 2022.
[36] R. Ding, F. Gao, and X. S. Shen, "3D UAV trajectory design and frequency band allocation for energy-efficient and fair communication: A deep reinforcement learning approach," *IEEE Trans. Wireless Commun.*, vol. 19, no. 12, pp. 7796–7809, Dec. 2020.
[37] E. Dahlman, S. Parkvall, and J. Skold, *5G NR: The Next Generation Wireless Access Technology*, 1st ed. Gainesville, FL, USA: Academic, 2018.
[38] R. Jain, D. Chiu, and W. Hawe, "A quantitative measure of fairness and discrimination for resource allocation in shared systems," Digit. Equip. Corp., Maynard, MA, USA, Tech. Rep. DEC-TR-301, Sep. 1984.

SHU MITSUI (Student Member, IEEE) is currently pursuing the M.S. degree with the Graduate School of Engineering, Tohoku University. His research interests include UAV communication networks, non-terrestrial communication networks, and wireless communication networks.

HIROKI NISHIYAMA (Senior Member, IEEE) received the M.S. and Ph.D. degrees in information science from Tohoku University, Japan, in 2007 and 2008, respectively. He is currently a Professor with the Graduate School of Engineering, Tohoku University. He has published more than 190 peer-reviewed papers, including many publications in the prestigious IEEE journals and conferences. His research interests include satellite communications, unmanned aircraft system networks, wireless and mobile networks, ad hoc and sensor networks, green networking, and network security. He is a Senior Member of the Institute of Electronics, Information, and Communication Engineers (IEICE). He has received Best Paper Awards from many international conferences, including IEEE's flagship events, such as the IEEE Global Communications Conference in 2014 (GLOBECOM'14), GLOBECOM'13, and GLOBECOM'10; the IEEE International Conference on Communications in 2018 (ICC'18), ICC'17, and ICC'16; and the IEEE Wireless Communications and Networking Conference in 2014 (WCNC'14) and WCNC'12. He was also a recipient of the Prizes for Science and Technology from the Ministry of Education, Culture, Sports, Science, and Technology, Japan, in 2018; the 2017 FUNAI Foundation's Academic Award for Information Technology; the 29th Advanced Technology Award for Creativity in 2015; the IEEE Communications Society's Asia–Pacific Board Outstanding Young Researcher Award 2013; and the IEICE Communications Society Academic Encouragement Award 2011. One of his outstanding achievements is Relay-by-Smartphone, which provides the possibility to share information among many people using direct device-to-device communication. He currently serves as the Secretary for the IEEE ComSoc Sendai Chapter.